Catalysis Today xxx (xxxx) xxx

Contents lists available at ScienceDirect

Catalysis Today

journal homepage: www.elsevier.com/locate/cattod

Scale-up of high-pressure F-T synthesis in 3D printed stainless steel microchannel microreactors: Experiments and modeling

Nafeezuddin Mohammad [a], Chiemeka Chukwudoro [b], Sujoy Bepari [c], Omar Basha [b,*], Shyam Aravamudhan [a], Debasish Kuila [a,c,**]

[a] Joint School of Nanoscience and Nanoengineering, North Carolina A&T State University, Greensboro, NC, USA
[b] Department of Chemical, Biochemical and Bioengineering, North Carolina A&T State University, Greensboro, NC, USA
[c] Department of Chemistry, North Carolina A&T State University, Greensboro, NC, USA

ARTICLE INFO

Keywords:
Cobalt bimetallic catalyst
Fischer-Tropsch Synthesis
3D printed Microchannel
Microreactor
Modeling of scaleup FT synthesis

ABSTRACT

Scale-up of Fischer-Tropsch (F-T) synthesis using microreactors is very important for a paradigm shift in the production of fuels and chemicals. The scalability of microreactors for F-T Synthesis was experimentally evaluated using 3D printed stainless steel microreactors, containing seven microchannels of dimensions 1000 μm × 1000 μm × 5cms. Mesoporous silica (KIT-6), with high surface area, containing ordered mesoporous structure was used to incorporate 10% cobalt and 5% ruthenium using a one-pot hydrothermal method. Bimetallic Co-Ru-KIT-6 catalyst was used for scale-up of F-T Synthesis. The performance of the catalysts was evaluated and examined for three different scale-up configurations (stand-alone, two, and four microreactors assembled in parallel) at both atmospheric pressure and 20 bar at F-T operating temperature of 240 °C using a syngas molar ratio (H_2:CO) of 2. All three configurations of microreactors yielded not only comparable CO conversion (85.6–88.4%) and methane selectivity (~14%) but also similar selectivity towards lower gaseous hydrocarbons like ethane, propane, and butane (6.23–9.4%) observed in atmospheric F-T Synthesis. The overall selectivity to higher hydrocarbons, C_5 + is in the range of 75–82% at 20 bars.

A CFD model was used to investigate the effect of different design features and numbering up approaches on the performance of the microchannel reactor. The effect of the reactor inlet, the mixing internals and the channel designs on the dead zone %, the quality index factor, the cooling requirement and the maximum dimensionless temperature within the microreactor were quantified. There is no significant effect of increasing the channel width on the microreactor performance and operation of the microchannel reactor at lower Nusselt number that results in higher CO conversion. Increasing the channel width reduced the maximum temperature exhibited in the channel. Finally, the effect of increasing the y/x stacking ratio, i.e. having more reactor units in parallel compared to series, was investigated. Increasing the y/x ratio increased the cooling requirement and the maximum dimensionless temperature increase within the unit decreased the productivity. To minimize the productivity losses, numbering up in series is the better approach; however further analysis must be done to delineate heat removal requirements.

1. Introduction

Over the past decade, significant work has been carried out for process intensification of Fischer-Tropsch (F-T) Synthesis with a focus on modular reactors technology (MRT) and catalysts. This has been primarily led by a growing number of technology companies. The motivation of this approach lies in the fact that the main components of a given plant, such as reactors, heat exchangers, separators, etc., only represent about 20% of the overall capital cost; whereas 80% of the cost is incurred by installation and commissioning, which includes pipe-study, structural support, civil engineering, etc. [1]. Consequently, major reductions in the equipment size, coupled preferably with a degree of telescoping of equipment function, such as reactor/heat exchanger unit, or combined distillation/condenser/re-boiler, could

* Corresponding author.
** Corresponding author at: Department of Chemistry, North Carolina A&T State University, Greensboro, NC, USA.
E-mail addresses: ombasha@ncat.edu (O. Basha), dkuila@ncat.edu (D. Kuila).

https://doi.org/10.1016/j.cattod.2021.09.038
Received 19 April 2021; Received in revised form 21 September 2021; Accepted 26 September 2021
Available online 30 September 2021

result in significant cost savings by eliminating the support structure, expensive foundations and long pipe runs.

The fuels derived by F-T synthesis remain an area of great research and commercial interest due to its ability to produce clean transportation fuels to meet increasing global demand. Microreactor technology is a new emerging chemical engineering platform that can enable modular reactors for multipurpose engineering applications. Microreactors exhibit substantial performance improvements over conventional reactors by enabling efficient integration of thermal and mass transport operations and minimizing operating variable gradients within the system, while also minimizing the financial risk of deployment [2–4]. However, successful scaling up of an F-T microreactor process to meet demands without losing key characteristics like product quality, catalyst activity, and selectivity towards desired products requires effective reactor design and scale-up strategy. A variety of scaleup approaches have been performed for F-T synthesis over the past few years in different types of microreactors [5–7,9]. All these studies indicate that the decrease in the feature size can have a significant effect on the process intensification of F-T synthesis [10]. Three scale-up approaches are considered and tested using both experimental work and Computational Fluid Dynamics (CFD) modeling. The first approach is numbering up the microreactors in parallel, and the overall flow of the reactants is divided into number of individual microreactor inlets at constant operating conditions like pressure, GHSV, temperature and syngas feed ratio. The schematic diagram for this approach is shown in Fig. 1.

The second approach involves arranging the microreactors in series as shown schematically, in Fig. 2. In this approach, a single stream of syngas is connected to the inlet of the microreactor. The product outlet is the inlet for the second microreactor, and the series can continue. This is generally adopted to collect the desired hydrocarbon cuts during F-T Synthesis and enables control over the residence time for the F-T process.

The third approach is based on careful sizing-up of the dimensions (enlarging dimensions) of the reactor system [11], while minimizing losses in intensification. In this approach, a critical mass parameter is introduced, which represents the maximum change in reactor dimensions that will maintain the microreactor's competitive advantage in terms of productivity against other commercially available technologies at different scales, as shown in Fig. 3. A slight increase in the microreactor dimensions can potentially have significant cost advantages, while making it easier to troubleshoot and modify the system.

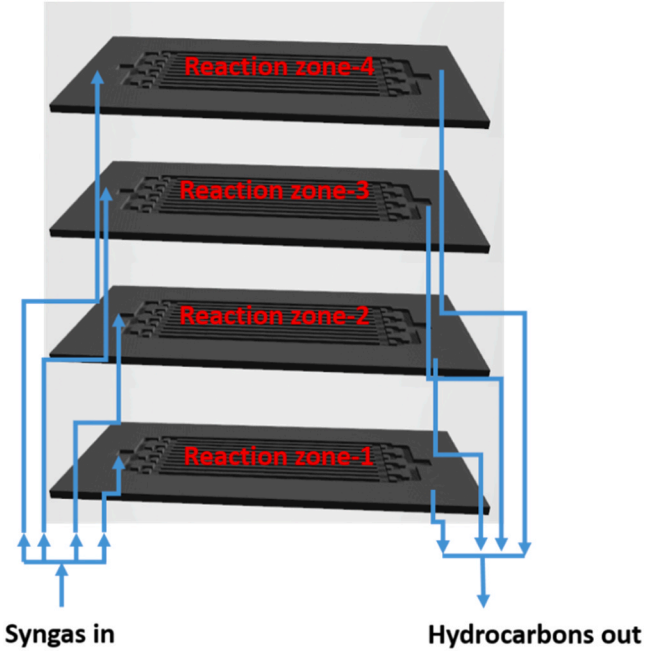

Fig. 1. Proposed Stacking of the microreactors in parallel.

In our experiments, we have considered the scale-up approach in parallel and demonstrated three reactor configurations: a) standalone reactor at high pressure, b) scale-up using two microreactors in parallel, and 3) scale-up using four reactors in parallel. The downstream operating conditions were monitored and productivity losses in terms of hydrocarbon selectivity, CO conversion, and deactivation studies of catalyst using all three approaches were determined.

In order to have a better understanding of our experimental studies, a multi-Eulerian CFD model was used to investigate microreactor performance for all the three numbering strategies previously mentioned and results were used to identify the best pathway.

2. Experimentation approach

2.1. Catalyst synthesis and loading

Our experimental work on F-T Synthesis in 3D printed stainless steel microchannel microreactor demonstrated high resistance to catalyst deactivation for Co-Ru-KIT-6 and better activity when compared to other six mesoporous silica catalysts in our previous studies [12,13]. Therefore, this catalyst was selected for the present scale-up experiments in high-pressure F-T synthesis. The details of catalyst preparation are presented elsewhere [14].

The Co-Ru-KIT-6 catalyst was loaded into the microchannels of the microreactor to maximize utilization of the free volume in the reaction zone. Then the reactor was packed with quartz wool followed by filtered gaskets at the inlet and outlet of the microreactor to create a leak-proof environment during the entire F-T Synthesis. For enhanced heat transfer and diffusivity, the catalyst was screened to a size of 150–200 μm. Once the catalyst is loaded, the weight of the microreactor before and after loading the catalyst gives the amount of catalyst used in the experiment. The microreactor inlet and outlet tubes were packed with quartz wool prior to sealing with ¼ inch Swagelok VCR filter gasket to prevent the catalyst from blowing into the reaction line. The microreactor loaded with the catalyst was carefully placed in the custom-built reactor block as shown in Fig. 4, and fitted into the reaction line using ¼ inch female Swagelok fitting.

2.2. Microreactor design and fabrication

To demonstrate the high-pressure Fischer-Tropsch Synthesis, the microreactor was modified at the inlet and outlet to ensure proper sealing at high pressure. Fig. 4 shows the AutoCAD design and the final 3D printed stainless steel reactor. As shown in Fig. 4, the cross-sectional view of the microreactor has seven microchannels between the cylindrical inlet and outlet. Each microchannel is 5 cm long, 1000 μm wide, and 1000 μm deep. The inlet and outlet of the microreactor have an outer diameter of ¼ inch Swagelok tubing that can perfectly align with a Swagelok filter to provide leak-proof sealing for high-pressure reactions.

2.3. Scale-up strategy and experiments

Three types of scale-up experiments were performed to demonstrate the scalability of microreactors for F-T Synthesis. The same catalyst and operating conditions were used for all the three reactor assemblies. The reactors used in this study are identical. The reaction conditions for this study are based on the optimum conditions obtained from our previous and preliminary experimental studies [13] ($T = 240$ °C and $P = 20$ bars). These conditions are designated as benchmark conditions for the rest of this work. The catalyst was first reduced ex-situ at 550 °C in a tubular furnace under the constant flow of 10% H_2/Ar before conducting the F-T experiments. To compensate the oxidation losses during the transfer of catalyst from the furnace into the microreactor, the catalyst is

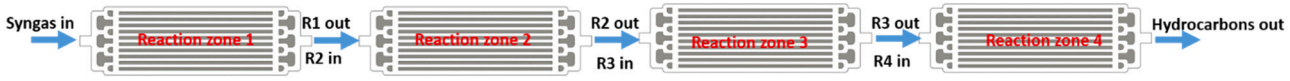

Fig. 2. Numbering up of microreactors in series.

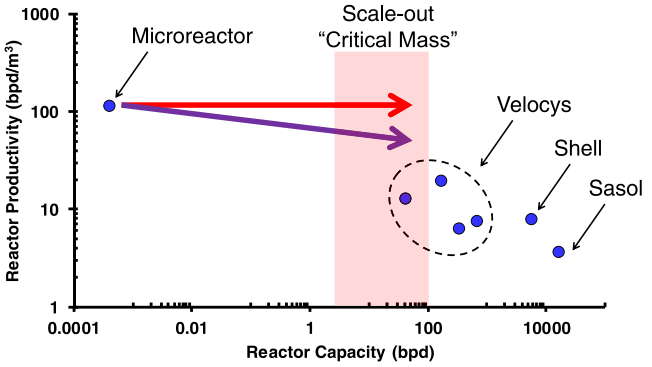

Fig. 3. Reactor Capacity vs Reactor Productivity for various F-T technologies.

again reduced in-situ at 350 °C for 4 h before starting the F-T experiments [15,16]. The F-T Synthesis was carried out at 240 °C with a constant syngas molar ratio of 2 (H_2:CO) and ~6000 GHSV. The pressure in the reaction line was monitored and maintained at 20 bars with nitrogen as the internal standard.

The first approach uses one microreactor with a single syngas inlet, and the hydrocarbon outlet with the catalyst between them termed as A-MR-1. The second type of microchannel microreactor assembly consists of two reactors in parallel, termed as A-MR-2. The syngas is divided into two inlets of the microreactor, and the products are combined after exiting individual outlets before leaving the reaction system.

The third type of reactor assembly is similar to the second reactor assembly which contains four microreactors arranged in parallel designated as A-MR-4. The syngas feed is divided into four inlets, and the hydrocarbons are combined at the outlet of each reactor before entering the product stream. The schematic diagram and the actual reactor assembly in the reaction line for F-T Synthesis are shown in Fig. 5. A typical reactor assembly with four microreactors in parallel, insulated with heating tapes connected to the F-T line, is shown in Fig. 6.

2.4. High pressure Fischer-Tropsch synthesis experimental setup

An *in-house* LabVIEW automated experimental setup is designed and demonstrated with accurate control over operating conditions (temperature, syngas flow rate, and pressure) for the high-pressure F-T reactions in microchannel microreactors. Fig. 7 shows the P&ID diagram of the overall high-pressure F-T Synthesis in a microreactor.

The flowrate for CO_2 enriched syngas (CO, H_2, CO_2, N_2 as carrier gas and internal standard) into the microreactor, which is embedded in a custom-built reactor block, is regulated using a pre-calibrated mass flow controller from Bronkhorst with minimum and maximum flowrates of 0.25 sccm and 20 sccm, respectively. The pressure in the reaction line is continuously measured and controlled using a back-pressure regulator obtained from Bronkhorst with maximum operating pressure of 30 bar. All the Bronkhorst digital devices are operated using FlowSuite that allows adjustments of in-built controllers, alarm, and counter settings with a graphical plot. The high-pressure equipment for F-T Synthesis is heated by different heating equipment obtained from Omega: a). The preheating for syngas and the temperature of the hot trap are monitored and controlled using a k-type thermocouple and heating tape. b) The reaction temperature is monitored by two thermocouples and is controlled by two heating cartridge heaters in the reactor block. Finally, the gaseous products along with carrier gas from the outlet of the microreactor are sent to the online GCMS system. The hot and cold traps to collect waxes and liquid hydrocarbons are maintained at 160 °C and 5 °C, respectively, for the entire F-T process. All the microdevices are connected to each other with a 1/8th Swagelok stainless steel tubing. Fig. 8 shows the pictorial view of overall microreactor experimental setup.

3. Modeling approach

3.1. CFD Model structure

An Eulerian CFD model was used to investigate the flow profiles within the microreactor. Fundamental balance equations for Eulerian CFD models are available extensively in the literature [18,19]. The RNG k-ε turbulence model [20] and the drag model of Ishii and Zuber [21] were used in this investigation. At the inlet of the reactor, Dirichlet velocity and volume fraction conditions for all phases are set, and a second order spatially accurate QUICK scheme [22–24] is employed to discretize all equations. Moreover, a multiphase variant of the SIMPLE scheme is used for pressure-velocity coupling [25]. The simulations were carried out using Fluent in Ansys Workbench V20. Furthermore, the kinetics by Anderson [26] were used to determine the CO consumption rate and a 2-α probability distribution model was used to describe the products distribution [27]. The vales for α_1 and α_2 were taken to be 0.659 and 0.941 [27].

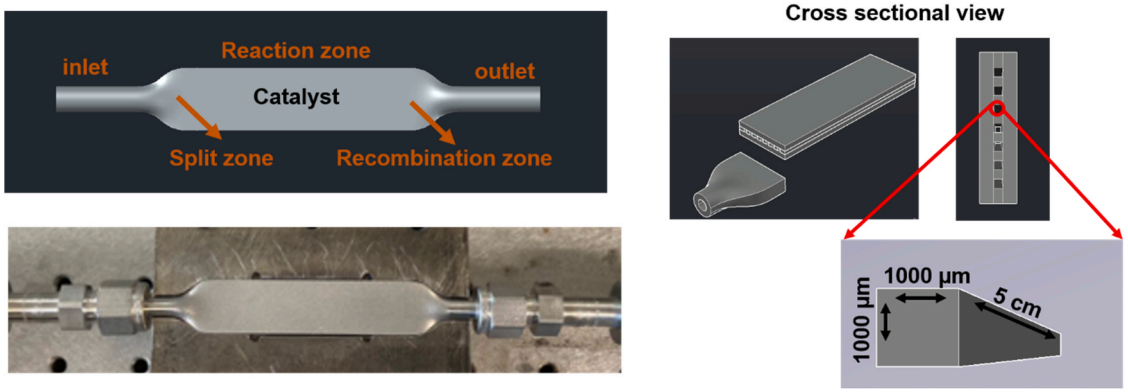

Fig. 4. AutoCAD design and the final 3D printed Stainless Steel microchannel microreactor.

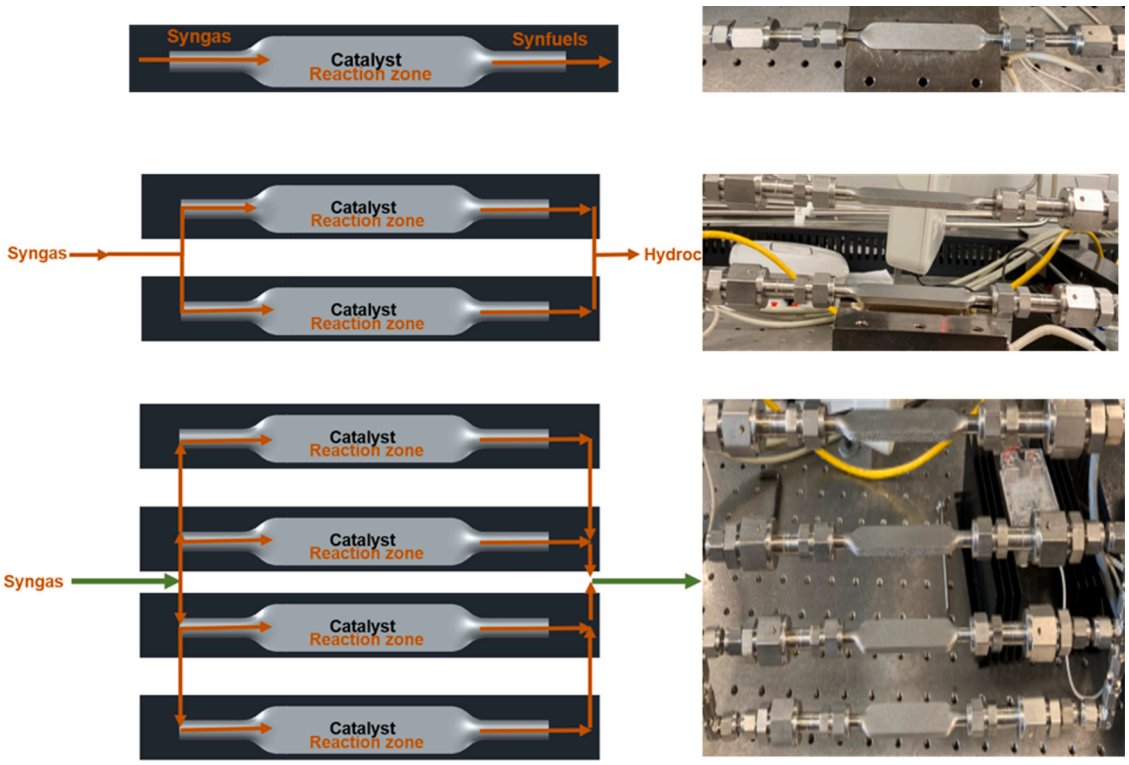

Fig. 5. Schematic diagram and the actual reactor assembly of scale-up experiments.

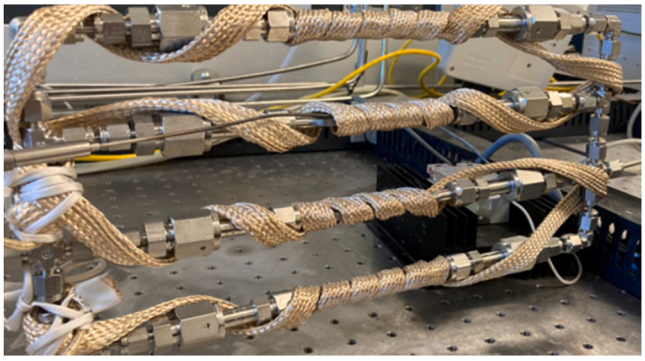

Fig. 6. A-MR-4 approach showing four microreactors arranged in parallel prior to insulation for F-T synthesis.

3.2. Microchannel reactor dimensions and operating conditions

The microchannel reactor dimensions are similar to that reported by Mohammad et al.[13], and a schematic is shown in Fig. 9. The microreactor is 12 mm wide and 41.23 mm in length and it contains 11 flow channels, 9 × 590 μm wide each; 2 (sides) x 836.3 μm wide, in addition to inlet and outlet flow distributors in the reactor. The overall free path coverage area of the microchannel reactor is 57.5%. Simulations were carried out at a temperature of 483 K, at pressures of 20 bar and inlet gas volumetric flow rate of 1 cc/minute.

3.3. Microchannel design variation methodology

The reactor design parameters that were investigated include the reactor inlet, the mixing shapes before the channels and the shapes of the channels. Figs. 10–12 show schematics of the different microreactor inlet designs, mixing shape designs and channel designs, respectively. With regards to the channel inlet, a straight inlet design (Fig. 10(a)), a T

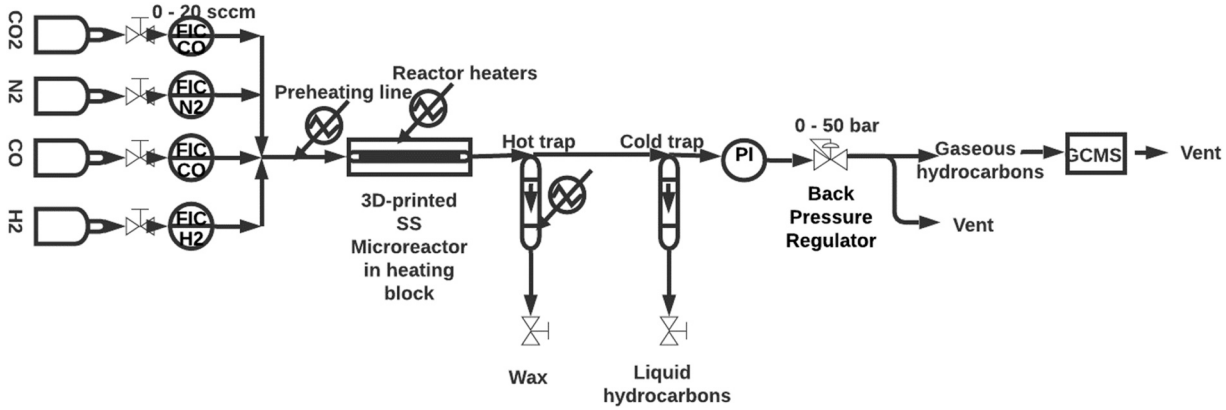

Fig. 7. The P&ID diagram of high-pressure F-T Synthesis.

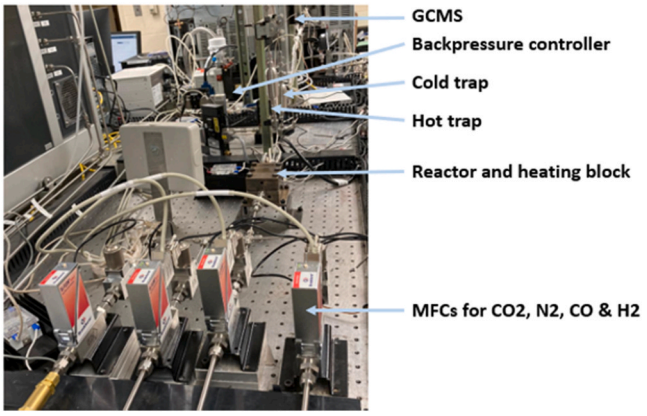

Fig. 8. Experimental setup for high pressure F-T synthesis using 3D printed SS Microreactors [17].

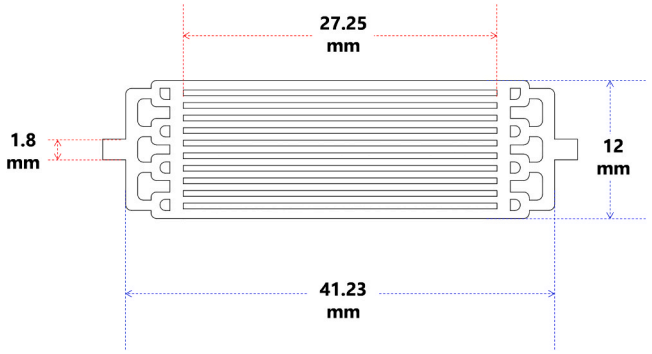

Fig. 9. Base case dimensions of the microchannel reactor.

inlet (Fig. 10(b)) and a V inlet (Fig. 10(c)), were investigated. In regard to the mixing shapes, three configurations were investigated as shown in Fig. 11; the first one is the original mixing internal design as shown in Fig. 11(a), the second one is a modified version of the original design without the central mixing (Fig. 11(b)) and the third one is a row of circular mixing elements, as shown in Fig. 11(c). The objective of varying the mixing elements was to investigate the effect of hindering the flow path and redistributing the incoming flow along the width of the rector on the overall flow profiles. Furthermore, 12 different flow channel designs were investigated, as shown in Fig. 6: the original straight channel with a width of 590 μm, 1: straight channel with a width of 750 μm, 2: includes rectangular mixing chambers with a straight connection between them, 3: includes rectangular mixing chambers with top/bottom alternating connections between them, 4: includes circular mixing chambers with a straight connection between them, 5: includes circular mixing chambers with top/bottom alternating

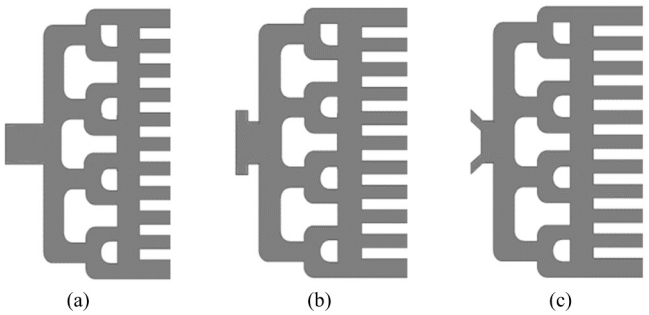

Fig. 10. Investigated design modifications of the microreactor inlet (a) straight inlet, (b) T-inlet, and (c) V-inlet.

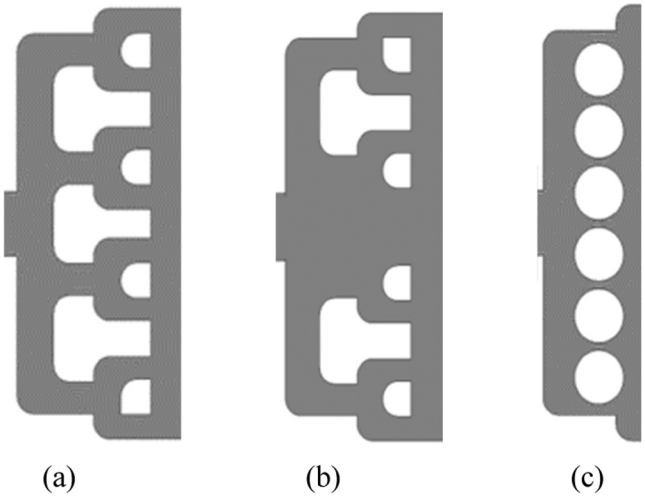

Fig. 11. Design modifications of the microreactor mixing shapes investigated: (a) original mixing, (b) modified mixing, and (c) circular mixing.

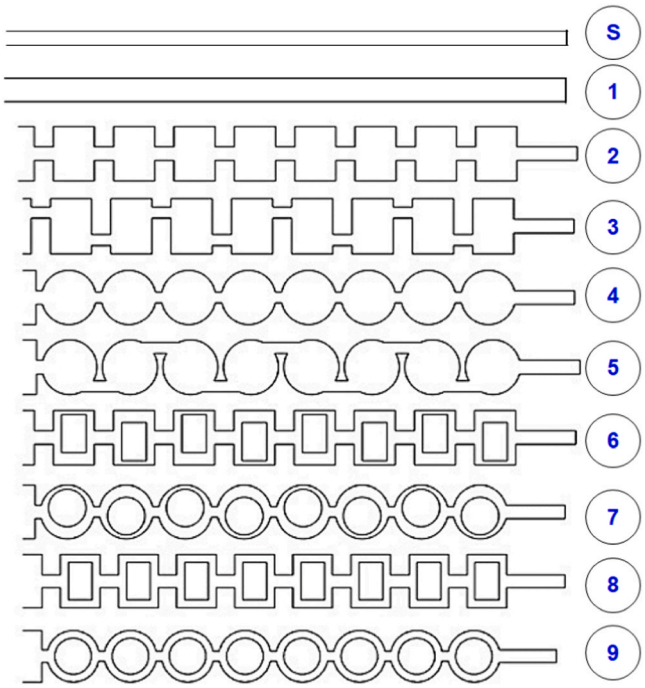

Fig. 12. Investigated channel designs in the microreactor [28].

connections between them, 6: includes rectangular mixing chambers with rectangular mixing elements within each chamber, the mixing elements were alternating off center, 7: similar to 6, but with circular mixing chambers and mixing elements, 8: similar to 6, with non-alternating rectangular mixing shapes within the rectangular chambers and 9: similar to 7, with non-alternating circular mixing shapes within the circular chambers.

The various combinations of inlet, mixing elements and channel configurations were modeled using the CFD model, with the objective of identifying the effect of increased tortuosity on mixing conditions and heat removal. Two primary parameters were used to characterize the design performance: the quality index factor (Eq. (1)) and the maximum dimensionless temperature increase (Eq. (2)). The quality factor is the fractional increase in flow over the microreactor between the maximum and minimum flow rates and is an indication of flow homogeneity throughout the unit. A quality index factor of zero means perfect

distribution, a value of 1 means no flow in at least one of the channels and a value over 1 implies there is a net backflow in at least one channel. The maximum dimensionless temperature indicates the peak temperature within the reactor and is used to compare the efficacy of heat removal of different thermal configurations or operating conditions within the reactor.

$$Q = \frac{m_{max} - m_{min}}{m_{max}} \quad (1)$$

$$\Delta T_{max} = \frac{T - T_w}{T_w} \frac{E_A}{RT_W} \quad (2)$$

3.4. Critical mass approach

As previously discussed, a critical mass analysis was performed. The effect of increasing the channel width from 0.5 mm to 0.75 mm was investigated. The effect of three operating conditions, characterized by Nusselt numbers (the ratio of convective to conductive heat transfer) of 4, 8 and 12, on the axial CO conversion and the temperature of the reactor were investigated. The changing Nusselt number can indicate either a change in the reactor material, the flow rate or nature of the cooling system or the presence of diluents in the feed.

3.5. Investigation of numbering up approach for scaling up microreactor systems

In this analysis, the effect of numbering up the microchannel reactors to produce 1 barrel per day, was investigated. Two primary configurations were tested, stacking in the x axis, which represents reactors in series, and stacking in the y axis, which represents stacking the reactors in parallel, as shown in Fig. 13. To achieve a capacity of 1 bpd, 2570 microreactor units are required, assuming no loss of productivity. The effect of the y/x stacking ratio was subsequently investigated using the CFD model on the: 1. Cooling requirement, 2. Maximum dimensionless temperature increase and 3. Overall system productivity for a 1 bpd unit.

4. Results and discussion

4.1. Experimental Results

4.1.1. Operating conditions over time on stream during F-T synthesis

One of the key advantages of using microreactor technology for a highly exothermic process like Fischer-Tropsch Synthesis is enhancement of heat and mass transfer when compared to that of conventional fixed bed reactors. This setup is monitored and investigated by acquiring data for operating conditions at every two hours for total duration of 72 h. The temperature in each reactor assembly is monitored using four k-type thermocouples and recorded for every two hours. The flowrate for nitrogen, carbon monoxide, and hydrogen was monitored and regulated by Flow Suite software acquired from Bronkhorst. The pressure in the reaction line is also controlled and monitored by the Flow Suite. Fig. 14 shows the graphical representation of all the operating conditions for 72 h of time on stream studies. To study the intrinsic effect of the stainless-steel material in the microreactor, F-T synthesis was also carried out with no catalyst in the reaction zone first. Neither CO conversion nor any peak for hydrocarbons was observed in the GCMS for control runs. These results confirm that the stainless-steel material is inert with the F-T reactants under F-T operating conditions.

4.1.2. Effect of scaling on catalyst performance

The scalability of microreactors was demonstrated by evaluating catalyst performance at the benchmark F-T operating conditions. F-T Synthesis was carried out at 240 °C with ~6000 GHSV using CoRu-KIT-6 with the three scale-up approaches using similar reaction parameters. The syngas ratio was maintained constant throughout the experiments

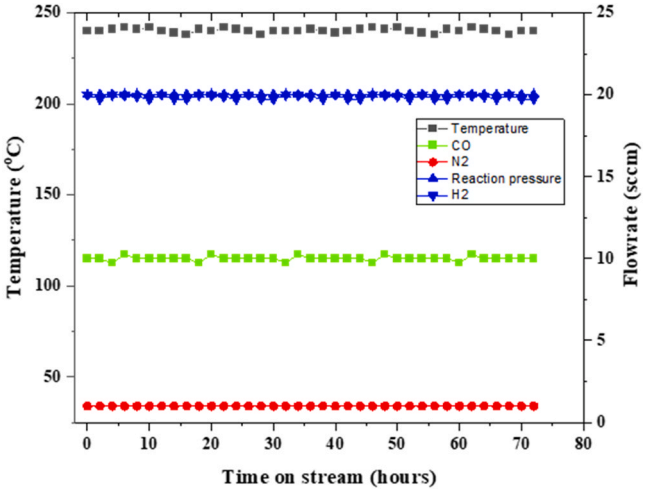

Fig. 14. Control Experiment for F-T synthesis at high-pressure operating conditions using the experimental setup: time on stream studies in the absence of any catalyst.

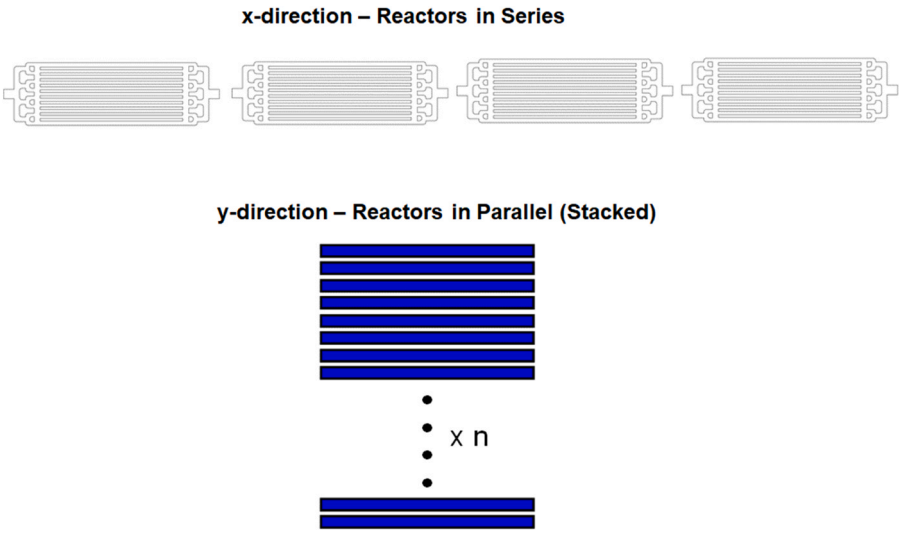

Fig. 13. Numbering up approach in the x (series) and y (parallel) directions.

(2 H_2:1CO) both at 1 bar and 20 bars. Two set of experiments were carried out using the scale up approach. The first set of reactions were carried out at 1 bar, 240 °C with syngas molar ratio of 2. The second set of reactions were carried out at 20 bar at a similar reaction temperature with same syngas feed ratio. Prior to F-T Synthesis, the catalyst was reduced in-situ in the presence of hydrogen to overcome the oxidation losses while loading the catalyst. Then, the reactors were cooled to room temperature and pressurized to the required operating pressure.

The performance of catalyst at 1 bar and benchmark operating conditions are shown in Fig. 15. For the A-MR-1 reactor, 77.41% of CO conversion was observed, while for A-MR-2 and A-MR-4, CO conversion was observed to be 75.71% and 78.17%, respectively. We observed no significant change in the selectivity towards hydrocarbons under these conditions for the reactions carried out in three reactors. When the F-T Synthesis was carried out at 1 bar, the catalyst yielded more methane, which is consistent with our previous F-T experiments conducted at atmospheric pressure [13–15].

The similar scale-up F-T experiments were conducted at 20 bar at benchmark operating conditions (240 °C, H_2: CO– 2:1) to demonstrate the scalability of microreactors for industrial F-T synthesis. The hydrocarbon selectivity and CO conversion for all three approaches in F-T Synthesis at 20 bars are shown in Fig. 16. An increase in CO conversion, 10 ± 1.5%, was observed for all the reactor configurations as the pressure was increased from 1 bar to 20 bars. The selectivity towards methane was averaged to almost 14 ± 2% in all three reactors.

The selectivity towards hydrocarbons and the CO conversion at these reaction conditions are listed in Table 1. All three microreactors assembly have not only shown comparable CO conversion and methane selectivity but also similar selectivity towards lower gaseous hydrocarbons like ethane, propane, butane. The higher hydrocarbons C_{5+} are observed in the range of 75–82%.

The data obtained from the three microreactor configurations serve as a proof of concept design for scaling up of F-T Synthesis by numbering up of the microreactors in parallel. To gain an in-depth understanding of the catalyst resistance towards the deactivation during F-T Synthesis, the performance of the catalyst in terms of CO conversion and the selectivity to methane was evaluated over 180 h of time on stream (TOS) studies. Fig. 17 shows the stability of the CoRu-KIT-6, indicating strong resistance towards deactivation. The results show that CO conversion was reasonably consistent for the first 40 h of F-T reaction. However, the conversion dropped from ~85% to ~74% between 40 and 85 h and maintained constant till 180 h of time on stream. The cause of deactivation for cobalt-based catalyst under these operating conditions is discussed elsewhere [12].

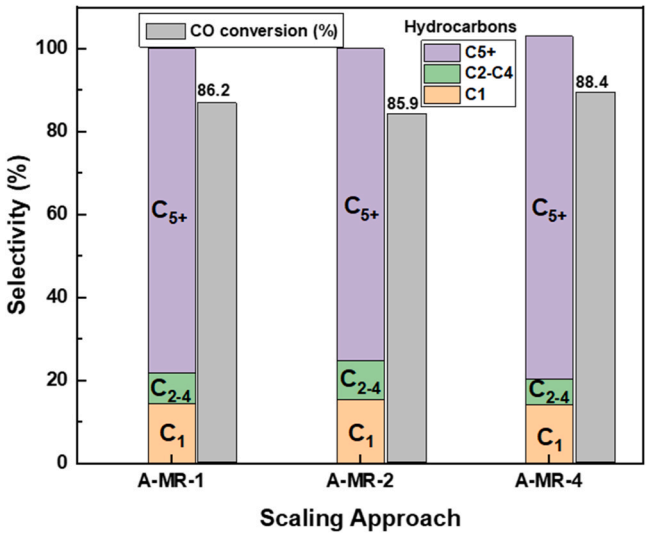

Fig. 16. Comparison of catalyst performance in three types of reactor assembly at 240 °C, H_2/CO (2), 20 bar, ~6000 GHSV.

Table 1
CO conversion and Selectivity for hydrocarbons at benchmark reaction conditions and 20 bars reaction pressure.

Reactor type	% Methane	% C_2-C_4	% C_{5+}	%CO conversion
A-MR-1	14.41	7.34	78.25	86.21
A-MR-2	15.36	9.4	75.24	85.6
A-MR-4	14.1	6.23	82.6	88.4

4.2. Modeling results

CFD simulation results of the base reactor design (Fig. 18) show both the velocity contours and velocity vector profiles throughout the microchannel reactor. In this figure, the dark blue areas represent areas of minimal gas flow, which are denoted as dead zones in this work: there is a significant dead zone percentage in this design, which can also be confirmed by taking a closer look at the velocity vector profiles. The dead zones represent areas of underutilized catalyst surface area, which

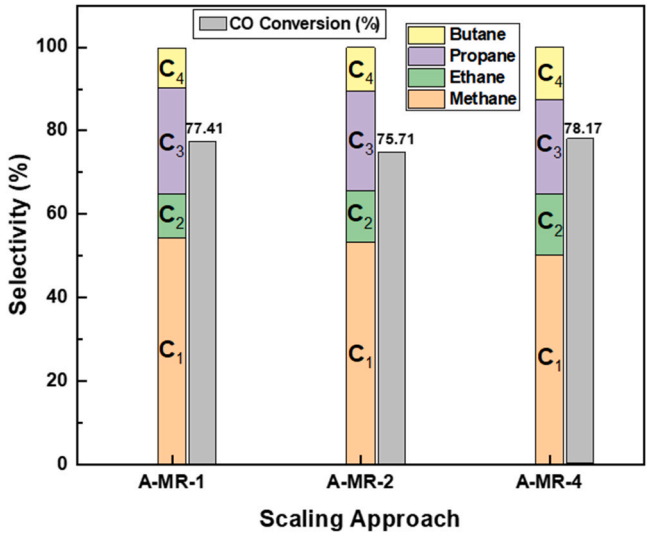

Fig. 15. Comparison of catalyst performance in three types of reactors assembly at 240 °C, H_2/CO (2), 1 bar, ~6000 GHSV.

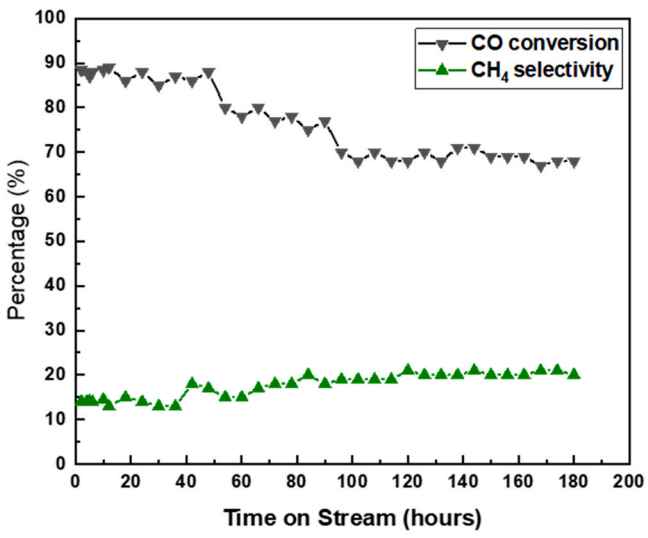

Fig. 17. Performance of catalyst in A-MR-4 microreactor assembly for 180 h of time on stream at benchmark reaction conditions and 20 bars.

prevents the unit from maximizing its productivity potential.

Figs. 19–26 show the CFD results for the effect of changing the inlet, mixing internals and channel designs on the velocity contours and velocity vector profiles within the microchannel reactors. As shown in Fig. 10, removing the large mixing internal facing the inlet of the microchannel reactor, results in better flow distribution for the straight inlet; whereas when a T inlet is introduced for the same case, the dead zone % increases, as shown in Fig. 20. Furthermore, when designing the reactor with a T-inlet, coupled with the original mixing internals, the dead zone % remains high, and is comparable to the original reactor design (Fig. 21). A similar result is shown when a V-inlet is used (Fig. 22).

Furthermore, Figs. 23–26 show CFD simulation results for the effect of changing the inlet channel design on the velocity contours and the velocity vector profiles within the microchannel reactor. Fig. 23 shows that the original mixing internals coupled with inverse circular channels significantly enhances the mixing within the channels, and reduces the dead zone%. A similar result is observed when using channels with box elements to allow for local recirculation of the gas (Fig. 24). On the other hand, introducing different mixing internals seems to have minimal effect on the flow profiles (Fig. 25) and similarly for using a T-inlet (Fig. 26). From these results, the primary governing design parameters to minimize the dead zone % within the microchannel reactors are the channel shapes, with higher tortuosity resulting in better mixing performance, followed by the inlet design, and finally the mixing internals near the inlet.

The results of all the simulations are compared in Tables 2–5. Table 2 compares the effect of all the different investigated designs on the dead zone % within the reactor. The channel types 5–9, represent the best performance, with the dead zone % reduced to less than 10% compared to original design, which had a dead zone % greater than 20%. Furthermore, Table 3 shows the effect of the different microchannel designs on the quality index factor; a quality index factor of zero means perfect distribution, a value of 1 means no flow in at least one of the channels and a value over 1 implies there is a net backflow in at least one channel. As can be seen in this table, the results mimic those of the dead zone %, with channel types 5–9 having significantly lower quality index factors, moreover, both the T-inlet and the V-inlet designs exhibited lower quality index factors compared to the straight inlet design.

In contrast, Table 4 shows the effect of the different designs on the cooling requirement in J within the microchannel reactor, and as can be seen channel types 6–9 performed significantly better compared to the others, with a significant reduction in the cooling requirements. This is primarily due to the enhanced mixing and uniform flow distribution within the system, which allows for a higher and more consistent heat removal driving force to be present. Moreover, the T-inlet design exhibited, and the Type 7 channel design exhibited superior performance.

Finally, Table 5 shows the effect of the microreactor design on the maximum dimensionless temperature increase, both channel designs 7–9 and the T-inlet design exhibited the best performance, which indicates that the temperatures in these designs are more uniform and their susceptibility to hotspot formation are much lower.

Fig. 27 shows the effect of increasing the channel width on the CO conversion along the microreactor length. The microreactor length was represented using the hydrodynamic residence time, to allow for comparison with other works in the literature and for performing dimensionless design analysis of the microreactor in the future., The overall conversion between the two-channel width was very similar, indicating that there is no significant effect of increasing the channel width on the microreactor performance. Moreover, operating the microchannel reactor at lower Nusselt number results in higher CO conversion. A lower Nusselt number corresponds to increasing the conductive heat transfer effects compared to convective effects; therefore, it can be inferred that operating the reactor at lower flow rates, while maximizing heat removal, will enhance the overall performance.

Fig. 28 shows the effect of increasing the channel width on the temperature along the microreactor length. Similar to Fig. 27, the microreactor length was represented using the hydrodynamic residence time, to allow for comparison with other works in the literature and for performing dimensionless design analysis of the microreactor in the future. As can be seen in this figure, increasing the channel width

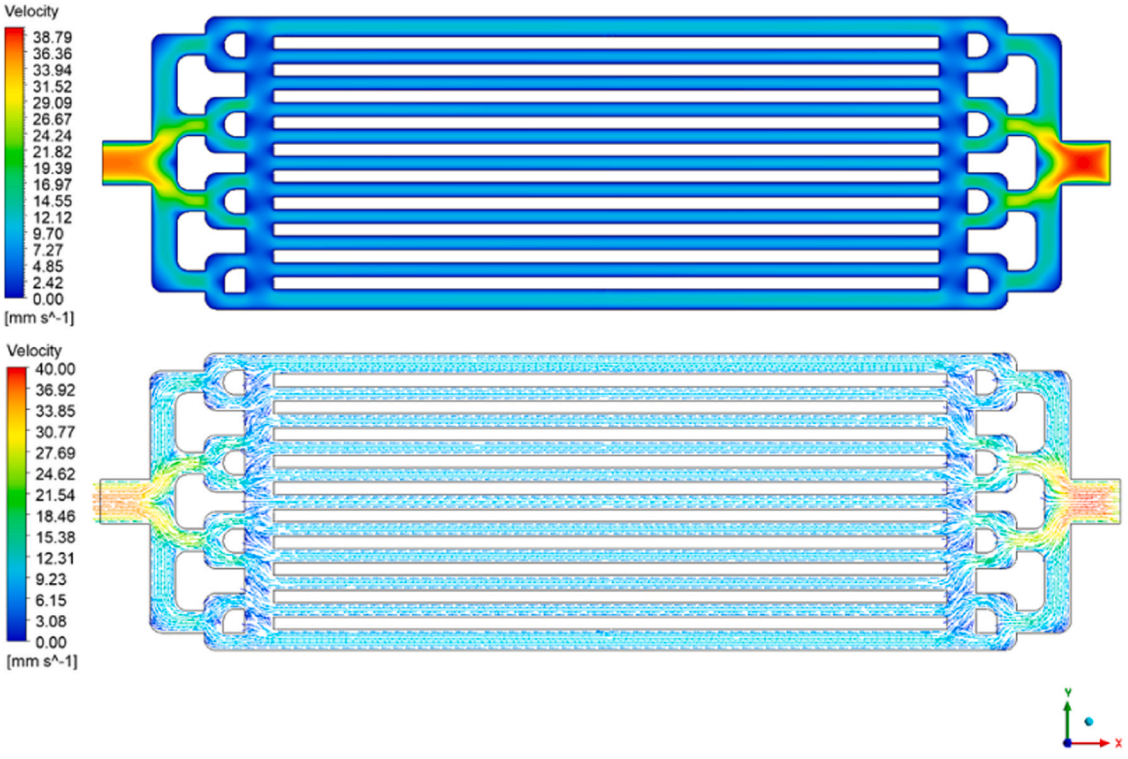

Fig. 18. Velocity contours (top) and velocity vector profiles (bottom) of the base case microreactor design.

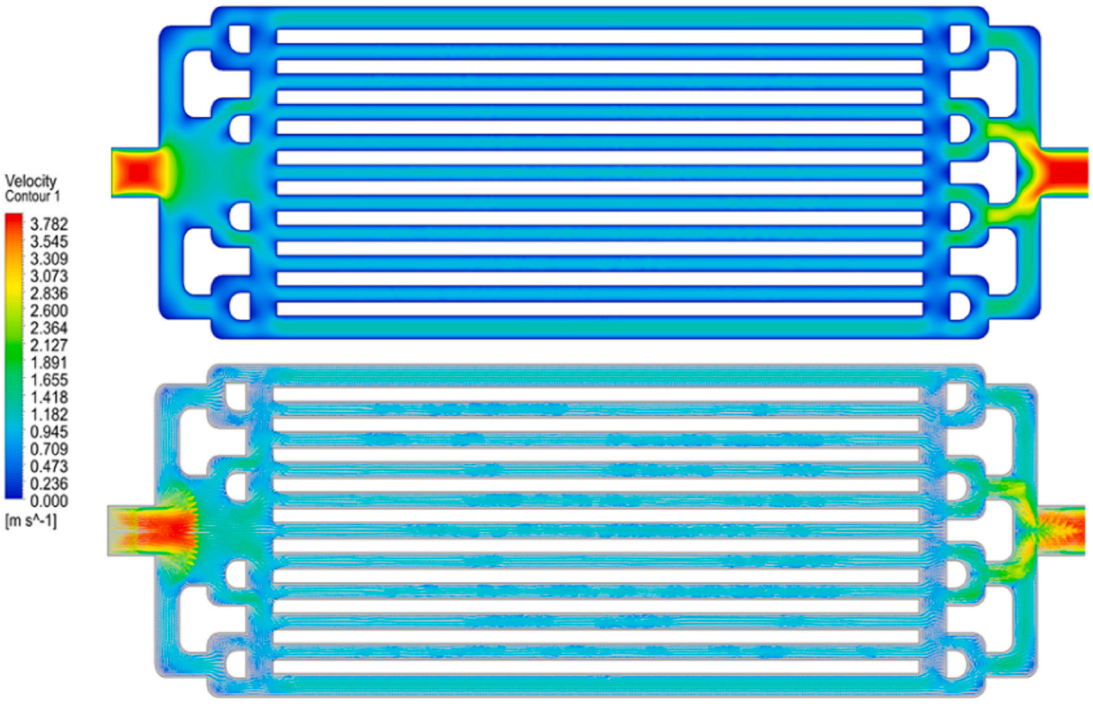

Fig. 19. CFD simulation results of effect of no mixing shape, coupled with a straight inlet: velocity contours (top) and the velocity vectors (bottom).

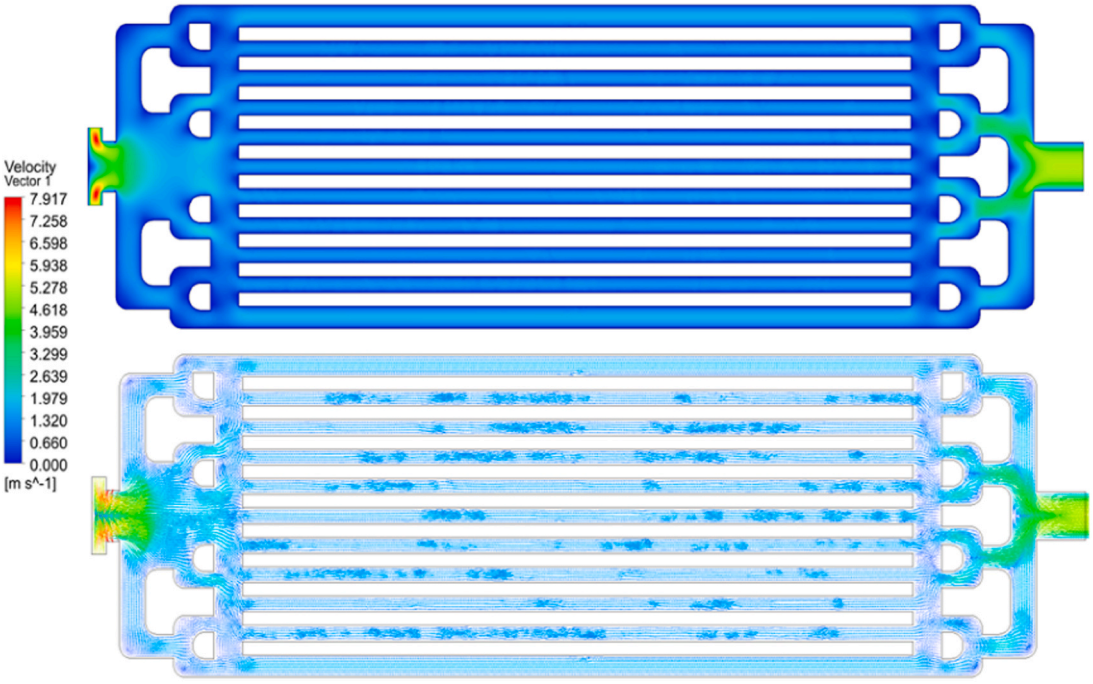

Fig. 20. CFD simulation results of effect of no mixing shape, coupled with a T-inlet: velocity contours (top) and the velocity vectors (bottom).

reduced the maximum temperature exhibited in the channel, which the 0.75 mm channel having a maximum temperature of 257 °C, compared to the 0.5 mm channel, which had a maximum temperature of 263 °C. However, both designs exhibited the same temperature profiles along the channel, with the maximum temperature observed at around 40% of the channel length. Moreover, similar to Fig. 27, operating the channel at lower Nusselt number increased the maximum temperature, which is due to higher CO conversion.

Fig. 29 shows the effect of changing the y/x stacking ratio on the cooling requirement of a 1 bpd unit consisting of 2570 microreactors. It is worthwhile to remember that stacking in the x axis represents reactors in series and stacking in the y axis represents stacking the reactors in parallel. As can be seen in Fig. 29, increasing the y/x stacking ratio significantly increases the cooling requirement of the microchannel reactor, which can be attributed to higher conversion and higher heat generation within the system. A y/x stacking ratio has a heating requirement which is almost 10 kJ higher compared to a stacking ratio of 0.1. Furthermore, when looking at the effect of the y/x stacking ratio

Fig. 21. CFD simulation results of effect of T-inlet and original mixing internals: velocity contours (top) and the velocity vectors (bottom).

Fig. 22. CFD simulation results of effect of V-inlet and original mixing internals": velocity contours (top) and the velocity vectors (bottom).

on the maximum dimensionless temperature increase (Fig. 30), a similar trend is observed, where the maximum dimensionless temperature increases as the y/x stacking ratio increases.

On the other hand, Fig. 31 shows the effect of increasing the y/x stacking ratio on the reactor productivity in bpd/m^3. Increasing the stacking ratio significantly decreases the reactor productivity. From these results it can be concluded that increasing the y/x stacking ratio, i.e. having more reactor units in parallel compared to series, will increase the cooling requirement and the maximum dimensionless temperature increase within the unit, and will decrease the productivity. Therefore, to minimize productivity losses, numbering up in series is the better approach; however, further analysis has to be done to delineate heat removal requirements.

4.3. Comparison with milli-structured reactors and scale-up potential

When comparing the above mentioned results in a microreactor to previously published analysis in milli-structured reactors, specifically those similar to the Velocys-type reactor, it is obvious that design considerations for appropriate axial sizing of milli- and micro- reactors remain unclear [29]. Velocys has reportedly increased the channel length from 178 mm at lab scale to 1000 mm for a commercial scale reactor [30], which is in agreement with the findings of this study that numbering up the reactors in series will enhance system productivity. Some of the factors to be considered, when scaling up processes containing such micro- or milli- reactors, while trying to maintain the very high reactor productivity and leverage the intensified transport gradients are:

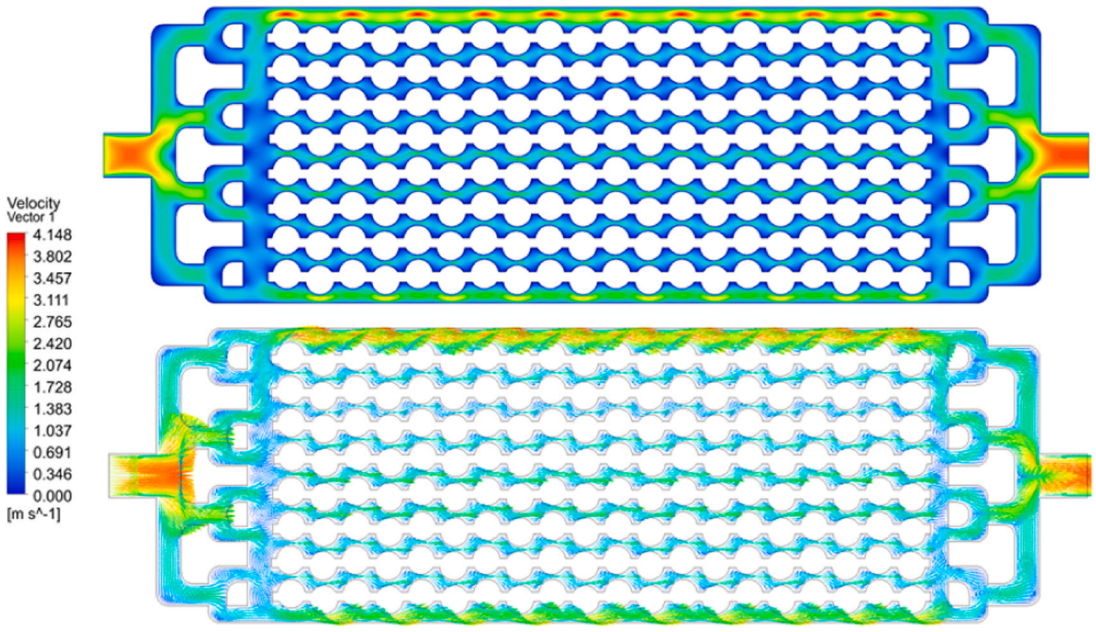

Fig. 23. CFD simulation results for the microreactor with a straight inlet, original mixing internals and channel design 4:: velocity contours (top) and the velocity vectors (bottom).

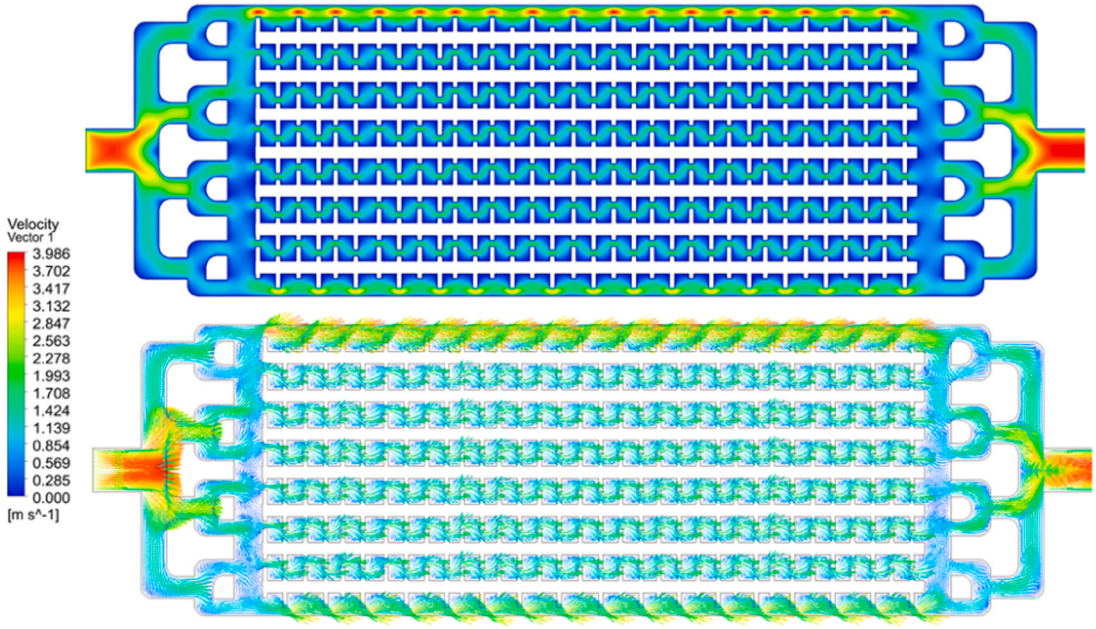

Fig. 24. CFD simulation results of the effect of the microreactor with a straight inlet, original mixing internals and channel design 3:: velocity contours (top) and the velocity vectors (bottom).

- Space velocity: Ideally, the space velocity should be kept constant throughout the system; this can be achieved by either reducing the number of parallel channels, which will directly enhance flow distribution, or through the introduction of mixing elements at the inlet of the reactor. The use and manipulation of mixing elements within the reactor can be more effectively achieved in microreactors compared to milli-structured ones. Other benefits of reducing the number of channels or reducing the number of micro-reactors in series lie in the simpler system design, which will allow for easier manufacturing, in addition to better ability to monitor and control the system.
- Catalyst deactivation rate: Theoretically, properly designed elongated microreactors should not have the drawback of significant temperature and concentration gradients when compared to milli-structured reactors. However, there will be some degree of catalyst deactivation in addition to thermal stresses on the reactor which increases the risk of mechanical failure. Furthermore, hotspot formation along the axial direction will occur if the reactor is operated counter currently, and may even occur when operated co-currently if the heat conduction along the reactor walls is not sufficient.
- Liquid holdup and pressure drop: Stemanic et al. [31,32] compared the liquid holdup between milli- and centi- scale fixed reactors, and determined liquid holdups of 6.71% and 4.65%, respectively. Liquid

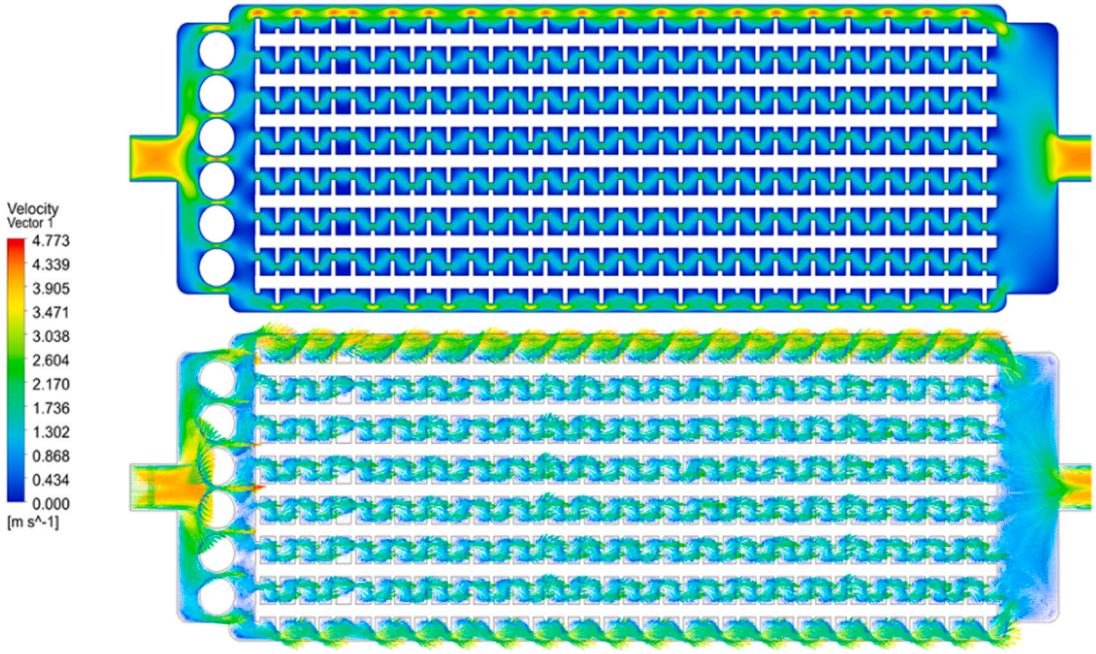

Fig. 25. CFD simulation results of the effect of the microreactor with a straight inlet, circular mixing internals and channel design 3: velocity contours (top) and the velocity vectors (bottom).

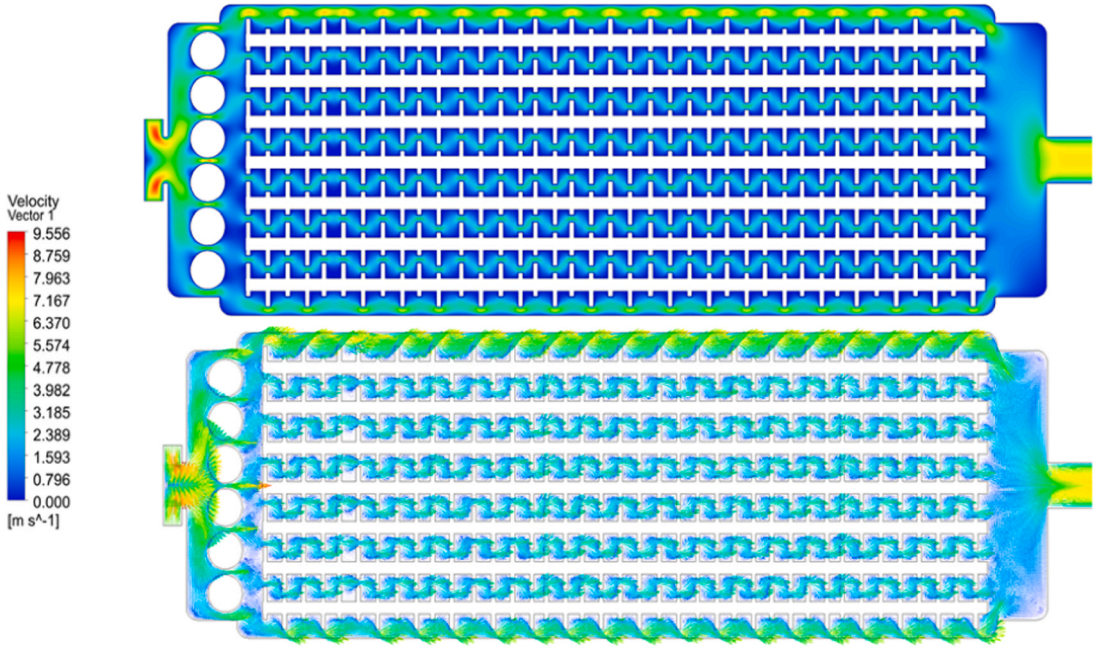

Fig. 26. CFD simulation results of the effect of the microreactor with a T-shaped inlet, circular mixing internals and channel design 3:: velocity contours (top) and the velocity vectors (bottom).

Table 2
Effect of different designs on the dead zone % within the microchannel reactor.

	Channel Design									
Inlet Design	**S**	**1**	**2**	**3**	**4**	**5**	**6**	**7**	**8**	**9**
Straight Inlet	24.7%	16.3%	11.9%	19.0%	9.9%	8.4%	6.9%	8.2%	7.4%	6.4%
T-Inlet	22.1%	13.7%	9.7%	17.0%	10.6%	8.0%	6.6%	6.2%	8.8%	8.6%
V-Inlet	22.8%	16.6%	11.4%	16.4%	10.7%	8.9%	6.2%	6.6%	9.1%	6.8%

Table 3
Effect of different designs on the quality index factor within the microchannel reactor.

	Channel Design									
Inlet Design	**S**	**1**	**2**	**3**	**4**	**5**	**6**	**7**	**8**	**9**
Straight Inlet	0.6	0.48	0.318	0.456	0.288	0.24	0.23	0.16	0.2	0.22
T-Inlet	0.35	0.252	0.168	0.294	0.137	0.11	0.09	0.14	0.1	0.1
V-Inlet	0.28	0.21	0.101	0.204	0.132	0.12	0.08	0.09	0.12	0.09

Table 4
Effect of different designs on the cooling requirement (J) within the microchannel reactor.

	Channel Design									
Inlet Design	**S**	**1**	**2**	**3**	**4**	**5**	**6**	**7**	**8**	**9**
Straight Inlet	17.7	12.92	6.903	12.21	6.726	6.73	6.2	4.96	7.61	6.2
T-Inlet	16.8	10.75	8.904	11.26	7.896	8.23	4.2	4.54	4.7	4.7
V-Inlet	17.43	13.42	8.018	12.72	8.192	5.23	6.45	4.36	7.32	6.97

Table 5
Effect of different designs on the maximum dimensionless temperature increase within the microchannel reactor.

	Channel Design									
Inlet Design	**S**	**1**	**2**	**3**	**4**	**5**	**6**	**7**	**8**	**9**
Straight Inlet	0.312	0.209	0.144	0.256	0.144	0.13	0.12	0.1	0.1	0.11
T-Inlet	0.243	0.175	0.104	0.16	0.092	0.12	0.06	0.06	0.07	0.09
V-Inlet	0.271	0.217	0.133	0.23	0.13	0.1	0.11	0.09	0.08	0.08

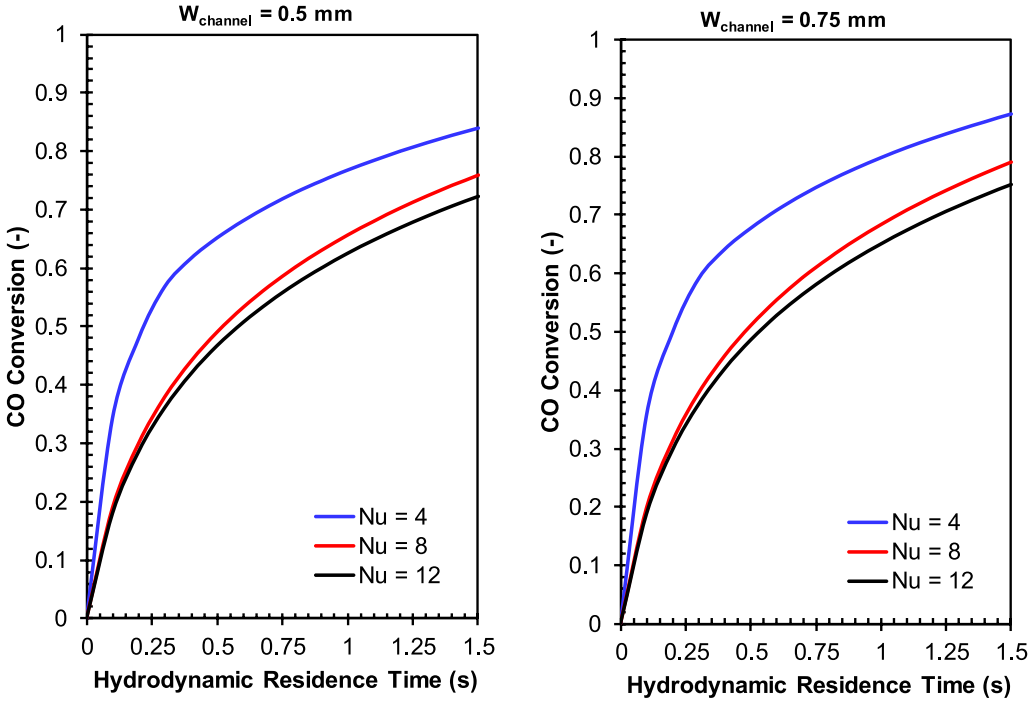

Fig. 27. Effect of increasing the channel width on the CO conversion along the channel length at three Nu values of 4, 8 and 12.

holdup is expected to increase with decreasing reactor dimensions, due to the higher formation of heavy hydrocarbons per reactor volume, coupled with lower liquid velocities. Liquid holdup may increase pressure drop along the reactor and can detrimentally affect the gas distribution and general flow profile within the unit.

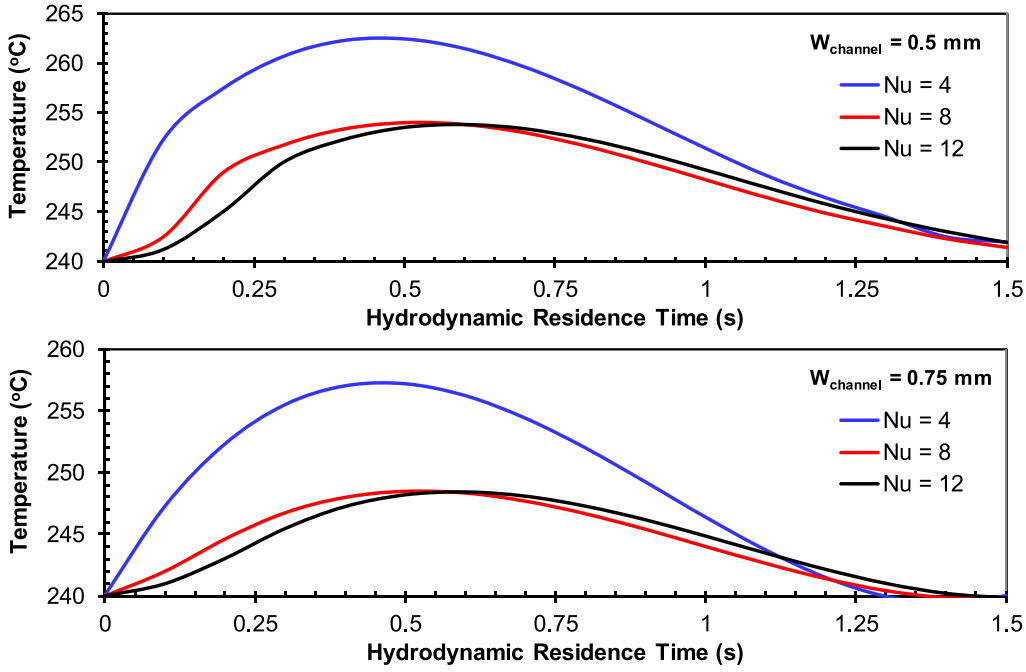

Fig. 28. Effect of increasing the channel width on the Temperature along the channel length at three Nu values of 4, 8 and 12.

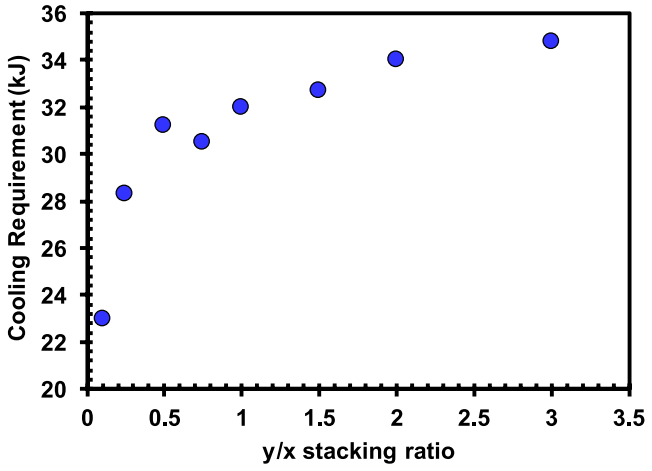

Fig. 29. Effect of changing the y/x stacking ratio on the cooling requirement within the numbered-up microreactor unit.

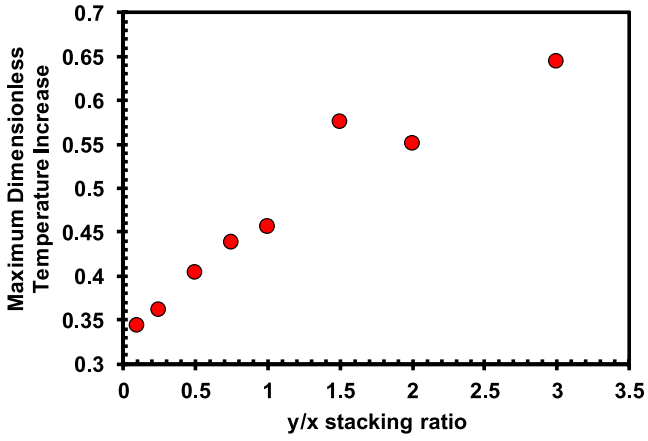

Fig. 30. Effect of changing the y/x stacking ratio on the maximum dimensionless temperature increase within the numbered-up microreactor unit.

5. Concluding remarks

The experiments for F-T Synthesis in microchannel microreactors were carried out using three types of parallel microreactor assembly to evaluate the scalability of microreactors. A highly active, CoRu-KIT-6, catalyst was synthesized using an one-pot hydrothermal method to test the reactor assembly for F-T Synthesis. The performance of each reactor assembly was found equivalent in terms of CO conversion and selectivity towards lower and higher hydrocarbons over 24 h of time on stream studies at 1 bar and 20 bars. The deactivation studies for the catalyst in the A-MR-4 assembly show that the catalyst was remarkably stable in terms of CO conversion until 180 h of time on stream with a ~11% drop in CO conversion. The operating conditions were also monitored for 72 h to access a microreactor's enhanced heat transfer effects for F-T Synthesis. The experimental conditions like reaction temperature, pressure, syngas mole ratio, and GHSV were maintained constant for all three microreactors to prove the adaptability of microreactors for scaling-up a F-T process. The workstation for high-pressure F-T reactions was successfully built as a proof of concept with three different scale-up configurations (stand-alone, two, and four microreactors assembled in parallel). The scalability of microreactors had no noticeable effect on catalyst performance in terms of CO conversion and the lower hydrocarbon selectivity at benchmark F-T operating conditions.

In order to investigate the effect of different design features on the performance of the microchannel reactor, an Eulerian CFD model was used. The effect of the reactor inlet, the mixing internals and the channel designs on the dead zone (%), the quality index factor, the cooling requirement and the maximum dimensionless temperature within the microreactor were investigated. Subsequently, an analysis was conducted to determine the effect of changing the channel dimensions and on the numbering up of the microchannel reactors to produce 1 bpd. Generally, channel types 5–9 showed the highest reduction of dead zone % within the microreactor, with the dead zone % reduced to less than 10% compared to original design, which had a dead zone % greater than

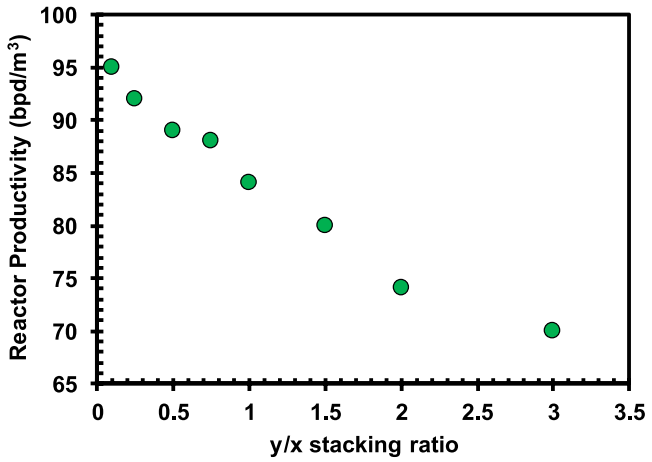

Fig. 31. Effect of changing the y/x stacking ratio on the productivity of the numbered-up microreactor unit.

20%. Moreover, there was no significant effect of increasing the channel width on the microreactor performance, and operating microchannel reactor at lower Nusselt number results in higher CO conversion. Increasing the channel width reduced the maximum temperature observed in the channel; while the 0.75 mm channel having a maximum temperature of 257 °C, compared to the 0.5 mm channel, which had a maximum temperature of 263 °C. However, both designs exhibited the same temperature profiles along the channel, with the maximum temperature observed at around 40% of the channel length. Additional analysis showed that increasing the y/x stacking ratio, i.e. having more reactor units in parallel compared to series, will increase the cooling requirement and the maximum dimensionless temperature increase within the unit, and will decrease the productivity. Therefore, it was concluded that in order to minimize productivity losses, numbering up in series is the better approach; however, further analysis has to be done to delineate heat removal requirements.

Declaration of Competing Interest

The authors declare that they have no known competing financial interests or personal relationships that could have appeared to influence the work reported in this paper.

Acknowledgements

The authors acknowledge the funding received from National Science Foundation-Center of Research Excellence in Science and Technology, USA (HRD #1736173) and The University of North Carolina System-Research Opportunities Initiative, USA (UNC-ROI 2017). This work was performed at North Carolina A&T State University and Joint School of Nanoscience and Nanoengineering, a member of Southeastern Nanotechnology Infrastructure Corridor (SENIC), which is supported by the National Science Foundation, USA (Grant ECCS-1542174). The authors also gratefully acknowledge Dr. Jeremy Feaster of Lawrence Livermore National laboratory for his support in designing the microreactor and his suggestions during the development of the high-pressure F-T experimental workstation.

References

[1] R. Zennaro, Fischer–Tropsch process economics. Greener Fischer-Tropsch Processes for Fuels and Feedstocks, Wiley-VCH Verlag GmbH & Co. KGaA,, 2013, pp. 149–169.
[2] G. Hunt, M. Torabi, L. Govone, N. Karimi, A. Mehdizadeh, Two-dimensional heat and mass transfer and thermodynamic analyses of porous microreactors with Soret and thermal radiation effects—an analytical approach, Chem. Eng. Process. - Process. Intensif. 126 (2018) 190–205. /04/01/ 2018.
[3] R.J.G.F.T.P. f F. Zennaro, Feedstocks. Fischer–Tropsch Process Economics, 2013, pp. 149–169.
[4] P. Piermartini, P. Pfeifer, Microreactor approaches for liquid fuel production from bioderived syngas −5 m3/h prototype development for HTHP water gas shift, Ind. Eng. Chem. Res. 54 (16) (2015) 4561–4571. /04/29 2015.
[5] C. Cao, J. Hu, S. Li, W. Wilcox, Y. Wang, Intensified Fischer–Tropsch synthesis process with microchannel catalytic reactors, Catal. Today 140 (3–4) (2009) 149–156.
[6] S.R. Deshmukh, et al., Scale-up of microchannel reactors for Fischer− Tropsch synthesis, Ind. Eng. Chem. Res. 49 (21) (2010) 10883–10888.
[7] P. Piermartini, T. Boeltken, M. Selinsek, P. Pfeifer, Influence of channel geometry on Fischer-Tropsch synthesis in microstructured reactors, Chem. Eng. J. 313 (2017) 328–335.
[9] M. Loewert, et al., Microstructured Fischer-Tropsch reactor scale-up and opportunities for decentralized application, Chem. Eng. Technol. 42 (10) (2019) 2202–2214.
[10] J. Lerou, A. Tonkovich, L. Silva, S. Perry, J. McDaniel, Microchannel reactor architecture enables greener processes, Chem. Eng. Sci. 65 (1) (2010) 380–385.
[11] P. Plouffe, M. Bittel, J. Sieber, D.M. Roberge, A. Macchi, On the scale-up of micro-reactors for liquid–liquid reactions, Chem. Eng. Sci. 143 (2016) 216–225. /04/02/ 2016.
[12] N. Mohammad, R.Y. Abrokwah, R.G. Stevens-Boyd, S. Aravamudhan, D. Kuila, Fischer-Tropsch studies in a 3D-printed stainless steel microchannel microreactor coated with cobalt-based bimetallic-MCM-41 catalysts, Catal. Today 358 (2020) 303–315. /12/01/ 2020.
[13] N. Mohammad, S. Bepari, S. Aravamudhan, D. Kuila, Kinetics of Fischer–Tropsch Synthesis in a 3-D printed stainless steel microreactor using different mesoporous silica supported Co-Ru catalysts, Catalysts 9 (10) (2019) 872.
[14] N. Mohammad, et al.. Fischer-Tropsch Synthesis in Silicon and 3D Printed Stainless Steel Microchannel Microreactors, 2021, p. 429.
[15] S. Bepari, X. Li, R. Abrokwah, N. Mohammad, M. Arslan, D. Kuila, Co-Ru catalysts with different composite oxide supports for Fischer–Tropsch studies in 3D-printed stainless steel microreactors, Appl. Catal. A: Gen. 608 (2020), 117838. /11/25/ 2020.
[16] S. Bepari, R. Stevens-Boyd, N. Mohammad, X. Li, R. Abrokwah, D. Kuila, Composite mesoporous SiO2-Al2O3 supported Fe, FeCo and FeRu catalysts for Fischer-Tropsch studies in a 3-D printed stainless-steel microreactor, Mater. Today.: Proc. 35 (2021) 221–228.
[17] N. Mohammad. Catalyst and Microreactor Development for Atmospheric and High-Pressure Fischer-Tropsch Synthesis, North Carolina Agricultural and Technical State University,, 2020.
[18] D.A. Drew, Mathematical modeling of two-phase flow, Annu. Rev. Fluid Mech. 15 (1) (1983) 261–291.
[19] D.A. Drew, S.L. Passman. Theory of Multicomponent Fluids, Springer,, New York, 1998.
[20] O.M. Basha. Computational Fluid Dynamics Modeling with Experimental Validation of the Complex Spatio-Temporal Phenomena In Slurry Bubble Column Reactors For Fischer-Tropsch Synthesis, Doctoral Dissertation, University of Pittsburgh,, 2016.
[21] M. Ishii, K. Mishima, Two-fluid model and hydrodynamic constitutive relations, Nucl. Eng. Des. 82 (2–3) (1984) 107–126.
[22] B.P. Leonard, Order of accuracy of QUICK and related convection-diffusion schemes, Appl. Math. Model. 19 (11) (1995) 640–653.
[23] B.P. Leonard, S. Mokhtari, Beyond first-order upwinding: the ultra-sharp alternative for non-oscillatory steady-state simulation of convection, Int. J. Numer. Methods Eng. 30 (4) (1990) 729–766.
[24] I. Ansys. Ansys CFX-Solver Theory Guide, ANSYS CFX Release, 2010, pp. 69–118.
[25] S.A. Vasquez and V.A. Ivanov, A phase coupled method for solving multiphase problems in unstructured meshes., Presented at the Proceedings of ASME FEDSM'00: ASME 2000 Fluids Engineering Division Summer Meeting, Boston, 2000.
[26] R.B. Anderson. Catalysis, P. H. Emmet,, New York, 1956.
[27] F. Arias Pinto, Master's Thesis. Investigating Microchannel Reactors for Fischer-Tropsch Synthesis, Department of Chemical and Petroleum Engineering, University of Pittsburgh,, 2016.
[28] M. Shaker, H. Ghaedamini, A.P. Sasmito, J.C. Kurnia, S.V. Jangam, A.S. Mujumdar, Numerical investigation of laminar mass transport enhancement in heterogeneous gaseous microreactors, Chem. Eng. Process.: Process. Intensif. 54 (2012) 1–11. /04/01/ 2012.
[29] C. Cao, D. Dang, Y. Li, J. Xu, Y. Cheng, Managing temperature uniformity of thermally integrated micro reformers with different axial dimensions: a detailed numerical study, Chem. Eng. Process. -Process. Intensif. 132 (2018) 218–228.
[30] A. Tonkovich, et al.. Improved Fischer-Tropsch Economics Enabled by Microchannel Technology, Velocys Technology, Plain City, OH, 2008.
[31] M. Stamenić, V. Dikić, M. Mandić, B. Todić, D.B. Bukur, N.M. Nikačević, Multiscale and multiphase model of fixed-bed reactors for Fischer–Tropsch synthesis: optimization study, Ind. Eng. Chem. Res. 57 (9) (2018) 3149–3162.
[32] M. Stamenić, V. Dikić, M. Mandić, B. Todić, D.B. Bukur, N.M. Nikačević, Multiscale and multiphase model of fixed bed reactors for Fischer–Tropsch synthesis: intensification possibilities study, Ind. Eng. Chem. Res. 56 (36) (2017) 9964–9979. /09/13 2017.